

hep-ph/9402233

UMN-TH-1233/94

UCSBTH-94-02

February 1994

Corrections to Bino Annihilation II: One-Loop Contribution to $\tilde{B}\tilde{B} \rightarrow Z^*$

Toby Falk,¹ Richard Madden,²
Keith A. Olive,² and Mark Srednicki¹

¹*Department of Physics, University of California, Santa Barbara, CA 93106, USA*

²*School of Physics and Astronomy, University of Minnesota, Minneapolis, MN 55455, USA*

Abstract

We calculate the one-loop contribution to the bino annihilation rate due to the process $\tilde{B}\tilde{B} \rightarrow Z^*$, which vanishes at tree level.

It is very likely that some extension of the standard electroweak model is needed. In fact, such an extension is probably dictated by cosmology in order to produce a baryon asymmetry and to provide a suitable dark matter candidate. The former typically relies on grand unification (though simpler extensions also work [1]), while the best motivated extension which provides a cold dark matter candidate is the minimal supersymmetric standard model (MSSM). Because of an unbroken discrete symmetry, R-parity, the lightest supersymmetric partner (LSP) is expected to be stable. This makes the LSP a natural candidate for the role of the non-baryonic dark matter. In previous studies, the lightest neutralino, a linear combination of the supersymmetric partners of the neutral $SU(2)$ gauge boson (neutral wino), $U(1)$ hypercharge gauge boson (bino), and the two neutral components of the Higgs doublets (higgsinos) has been suggested as the most likely candidate for the LSP [2]. In a large portion of parameter space, the least massive eigenstate is a nearly pure bino [3].

Neutralino annihilation rates have been calculated previously at tree level, under a variety of assumptions and to various degrees of accuracy [2, 4, 3, 5, 6, 7, 8, 9, 11]. For neutralinos which are nearly pure bino, the rate is dominated by creation of fermion pairs via the exchange of a sfermion, though many of the calculations have included annihilation channels into Higgs scalars as well. Since binos are $SU(2) \times U(1)$ singlets, they do not couple directly to the Z . Thus, s-channel annihilations through Z exchange which are very important for massive neutrino annihilations or higgsino co-annihilations [10, 11], do not occur for pure binos. Of course in reality the LSP is never a “pure” bino, but rather always contains some small admixture of higgsinos as well. Annihilations through Z exchange due to this admixture make a small contribution to the cross-section. In this paper, we consider a correction to the bino annihilation rate from the process $\tilde{B}\tilde{B} \rightarrow Z^*$, via the loop diagrams shown in fig. (1). Generically, the corrections are found to be much larger than the corrections due to the higgsino admixture. However, their contribution to the total annihilation cross-section remains small, on the order of a few percent or less over the physically allowed range of parameters. Recently one-loop corrections to the neutralino masses have been computed [12], and found to be very small (less than one per cent) in the parameter range of interest here. These corrections to the masses would make similarly small corrections to the annihilation cross section, and so are significantly smaller than those we compute here.

In general, the lightest neutralino mass eigenstate is a linear combination of the gauginos \tilde{W}^3 and \tilde{B} , and the higgsinos \tilde{H}_1^0 and \tilde{H}_2^0 :

$$\tilde{\chi}^0 = \alpha \tilde{W}^3 + \beta \tilde{B} + \gamma \tilde{H}_1^0 + \delta \tilde{H}_2^0 . \quad (1)$$

In the pure bino region ($\beta \simeq 1$), $m_{\tilde{\chi}^0} \simeq M_1$, where M_1 is the supersymmetry breaking $U(1)$ gaugino mass. For our purposes here, the supersymmetric parameter space can be described by one additional parameter, ε , the supersymmetric Higgs mixing mass (often denoted by $-\mu$). In the bino region, results are very insensitive to the ratio of Higgs vevs, $\tan \beta$ ($\tan \beta$ should not be confused with the β in eq. (1)). In what follows we have chosen $\tan \beta = 2$ and assumed a top quark mass of 160 GeV. We simplify by using GUT boundary conditions to relate M_2 , the $SU(2)$ gaugino mass, to M_1 via $M_1 = \frac{5}{3}M_2 \tan^2 \theta_w$. From here on, we will assume that $\varepsilon \gg M_2$ so that we are working in the nearly pure bino region and write $m_{\tilde{\chi}^0} = m_{\tilde{B}}$.

We begin by calculating the annihilation rate of almost pure binos to fermion anti-fermion pairs $\bar{F}F$ via (1) t-channel sfermion exchange, (2) $\tilde{B}\tilde{B} \rightarrow Z^* \rightarrow \bar{F}F$ via the loop diagrams of fig. (1), and (3) $\tilde{B}\tilde{B} \rightarrow Z^* \rightarrow \bar{F}F$ via the small but non-zero admixture of \tilde{H}_1^0 and \tilde{H}_2^0 in $\tilde{\chi}^0$ (see eq. (1)).

The relevant interaction terms are

$$\begin{aligned} \mathcal{L} = & -\frac{g_2}{4 \cos \theta_w} Z_\mu \left(\overline{\tilde{H}}_1^0 \gamma^\mu \gamma_5 \tilde{H}_1^0 - \overline{\tilde{H}}_2^0 \gamma^\mu \gamma_5 \tilde{H}_2^0 \right) + \sum_f \left\{ \frac{g_1}{\sqrt{2}} \bar{f} (Y_{f_R} \tilde{f}_R P_- + Y_{f_L} \tilde{f}_L P_+) \tilde{B} + \text{h.c.} \right. \\ & \left. + \frac{g_2}{\cos \theta_w} Z_\mu \left[\bar{f} \gamma^\mu (C_V^f - C_A^f \gamma_5) f + i (C_V^f + C_A^f) (\tilde{f}^* \partial^\mu \tilde{f} - \tilde{f} \partial^\mu \tilde{f}^*) \right] \right\} \end{aligned} \quad (2)$$

where $P_\pm = (1 \pm \gamma_5)/2$, $Y_{f_R} = 2Q_f$, $Y_{f_L} = 2(Q_f - T_3^f)$, $C_V^f = -T_3^f/2 + Q_f \sin^2 \theta_w$, and $C_A^f = -T_3^f/2$. The fermion charge is denoted by Q_f , and $T_3^f = +1/2$ for up-type quarks and neutrinos, and $-1/2$ for down-type quarks and charged leptons. The sum runs over all fermions. We neglect the effect of sfermion mixing, which is treated in detail in ref. [9].

To derive a thermally averaged cross section, we make use of the technique of ref. [13]. We expand $\langle \sigma v_{\text{rel}} \rangle$ in a Taylor expansion in powers of $x = T/m_{\tilde{B}}$:

$$\langle \sigma v_{\text{rel}} \rangle = a + bx + O(x^2) . \quad (3)$$

The coefficients a and b are given by

$$\begin{aligned} a &= \sum_F v_F \tilde{a}_F \\ b &= \sum_F v_F \left[\tilde{b}_F + \left(-3 + \frac{3m_F^2}{4v_F^2 m_{\tilde{B}}^2} \right) \tilde{a}_F \right] \end{aligned} \quad (4)$$

where the subscript F specifies the final state fermions, \tilde{a}_F and \tilde{b}_F are computed from the expansion of the matrix element squared in powers of p , the incoming bino momentum, and

$v_F = (1 - m_F^2/m_{\tilde{B}}^2)^{1/2}$ is a factor from the phase space integrals. In terms of the squared reduced transition matrix element $|\mathcal{T}|^2$, \tilde{a}_F can be written simply as,

$$\tilde{a}_F = \frac{1}{32\pi} \frac{1}{m_{\tilde{B}}^2} |\mathcal{T}_F(p=0)|^2 \quad (5)$$

Denoting the reduced transition amplitudes for the processes (1), (2) and (3) listed above by $\mathcal{T}_{\text{sfex}}$, $\mathcal{T}_{\text{loop}}$ and \mathcal{T}_{mix} respectively, we have

$$|\mathcal{T}_F| = |\mathcal{T}_{\text{sfex}} + \mathcal{T}_{\text{loop}} + \mathcal{T}_{\text{mix}}|, \quad (6)$$

where

$$\mathcal{T}_{\text{sfex}}(p=0) = \frac{g_1^2}{2} (Y_{F_L}^2 + Y_{F_R}^2) \frac{m_F m_{\tilde{B}}}{m_{\tilde{B}}^2 - m_F^2 + m_F^2} \quad (7)$$

$$\mathcal{T}_{\text{mix}}(p=0) = -2 \left(\frac{g_2}{\cos \theta_w} \right)^2 C_A^F \frac{m_F m_{\tilde{B}}}{m_Z^2} (\gamma^2 - \delta^2) \quad (8)$$

$$\begin{aligned} \mathcal{T}_{\text{loop}}(p=0) &= + \frac{2g_2}{\cos \theta_w} C_A^F \frac{m_F m_{\tilde{B}}}{m_Z^2} \frac{g_1^3}{\sin \theta_w} \frac{1}{32\pi^2} \times \\ &\quad \sum_f \left\{ Y_{f_L}^2 [2(T_3^f - Q_f \sin^2 \theta_w) - T_3^f I_f] + Y_{f_R}^2 [2Q_f \sin^2 \theta_w - T_3^f I_f] \right\} \\ &= - \frac{2g_2}{\cos \theta_w} C_A^F \frac{m_F m_{\tilde{B}}}{m_Z^2} \frac{g_1^3}{\sin \theta_w} \frac{1}{32\pi^2} \sum_f T_3^f (Y_{f_L}^2 + Y_{f_R}^2) I_f \end{aligned} \quad (9)$$

and where

$$I_f = \int_0^1 dr \int_{-r}^r ds \frac{m_f^2}{(m_f^2 - m_{\tilde{f}}^2 - m_{\tilde{B}}^2) r + m_{\tilde{B}}^2 s^2 + m_{\tilde{f}}^2 + i\varepsilon}. \quad (10)$$

Here C_A^F , Y_{F_L} , Y_{F_R} are the quantum numbers of the final state fermion, and m_F and $m_{\tilde{F}}$ are the masses of the final state fermion and its supersymmetric partner. These expressions for the amplitudes do not include spin dependence, but we note that they will vanish if either the binos or fermions are spin parallel. In the other cases the amplitudes are antisymmetric under exchange of spins in the incoming or outgoing states. So their relative signs remain the same allowing us to directly sum and average over spin states giving eq. (5). To compute \tilde{b}_F , where we need to consider $p \neq 0$, this simple spin dependence no longer holds and we use standard trace techniques to calculate the squared transition matrix element.

To compare the relative effect of the loop and the higgsino mixing diagrams on the dominant sfermion exchange process, we need to find the \tilde{a}_F and \tilde{b}_F coefficients for 1) the sfermion exchange alone, 2) the sfermion exchange plus the loop diagram and 3) the sfermion

exchange plus the higgsino mixing diagram. The \tilde{a}_F for each combination can be read off from eq. (5) by redefining \mathcal{T}_F to contain different combinations of diagrams, but the \tilde{b}_F will need to be separately computed in each case. The expressions are too complicated to reproduce here.

We now discuss the effect of this loop correction on the relic density and detectability of binos. In fig. (2), we show a contour plot of $\Omega_{\tilde{B}} h^2$ as a function of $m_{\tilde{B}}$ and the common sfermion mass $m_{\tilde{F}} = m_{\tilde{F}}$, assuming that binos annihilate to fermions only through the sfermion exchange process (1). $\Omega_{\tilde{B}}$ is the mass density of the binos in units of the critical density, and h is the Hubble parameter in units of $100 \text{ km s}^{-1} \text{ Mpc}^{-1}$. The region where $m_{\tilde{F}} > m_{\tilde{B}}$ is excluded, since here the LSP would be a sfermion rather than the bino. Notice the effect of the top threshold at $m_{\tilde{B}} = 160 \text{ GeV}$. Because the cross-section is p-wave suppressed, we have $a_F \propto (m_F^2/m_{\tilde{B}}^2)$, and so as we cross below $m_{\tilde{B}} = m_{\text{top}}$ the relic density rises sharply. Notice also that $\Omega_{\tilde{B}} h^2 \leq 1$ requires $m_{\tilde{F}} \lesssim 500 \text{ GeV}$, while $\Omega_{\tilde{B}} h^2 \leq 1/4$ requires $m_{\tilde{F}} \lesssim 350 \text{ GeV}$. Keep in mind that these are approximate values for $\Omega_{\tilde{B}} h^2$ as only the dominant part of the cross-section was used here, though the corrections are very small.

In fig. (3), we compare the effect of including the loop diagrams (2) on the relic density of binos $\Omega_{\tilde{B}} h^2$ to the effect of including the higgsino mixing diagram (3). As ε gets larger, the admixture of higgsino in $\tilde{\chi}^0$ gets smaller, and so does the prefactor $(\gamma^2 - \delta^2)$ in eq. (8) (and in the corresponding $p \neq 0$ expression). In the exactly pure bino limit, corresponding to $\varepsilon \rightarrow \infty$ at fixed M_1 , the process $\tilde{\chi}^0 \tilde{\chi}^0 \rightarrow Z$ is forbidden, as mentioned above. For each point in the $m_{\tilde{B}} - m_{\tilde{F}}$ plane we find the value of ε at which the magnitude of the loop correction is equal to that of the higgsino mixing correction. We then plot several contours of these ε values. For each ε , it is the region to the left of the corresponding contour where the loop effect is greater. In the parameter range of interest, we find that the loop correction to $\Omega_{\tilde{B}} h^2$ vanishes near the line $m_{\tilde{F}} = m_{\tilde{B}}$, which is why ε tends toward large values there. For the moderate values of $m_{\tilde{F}}$ represented in fig. (3), we see that the effect of the loop is larger than the effect of higgsino mixing for large ranges in $m_{\tilde{B}}$ in the pure bino regime. Again, we exclude the region where $m_{\tilde{B}} > m_{\tilde{F}}$. We also exclude the region below the top threshold where both diagrams have a negligible effect on $\Omega_{\tilde{B}} h^2$.

Although we have found that for a large portion of the parameter space the loop correction is larger than the commonly used correction due to a higgsino admixture, the net effect on the annihilation cross-section and ultimately on $\Omega_{\tilde{B}} h^2$ is small. For all values of $m_{\tilde{F}}$ and M_2 consistent with $\Omega_{\tilde{B}} h^2 \leq 1$, the effect is at most a few percent, and in the allowed region, the effect predominantly decreases the relic density. Below the top threshold, the effect of the

loop diagrams drops by a factor of ~ 300 due to the accumulation of a number of unrelated factors. (This is also true for the higgsino mixing diagram.) Of course in the very thin slice of parameter space near $m_{\tilde{B}} = m_Z/2$, the annihilation cross-section will be greatly enhanced, and the effect of the loop diagrams will be significant. Because this effect is limited to a small region of parameter space we do not consider it further. We note only that in such regions the expansion of the thermal average should be done as explained in ref. [10].

In addition to the effect of the loop correction on the relic density, it is also of interest to compute the effect on the zero temperature annihilation cross-section ($p = 0$) which governs annihilations in the galactic halo. Indeed, galactic halo LSP annihilation products have been frequently discussed as a potential signatures for dark matter [14].

In fig. (4), we show the effect of the loop diagrams on the zero-temperature cross-section, $\langle \sigma v_{\text{rel}} \rangle$, at $\varepsilon = \infty$. The contours show the percentage change in a due to the inclusion of the loop correction diagrams (2). The effect is larger than on the relic density, but in the physically allowed region the effect is still $\lesssim 11\%$. We again see the top threshold at $m_{\tilde{B}} = 160$ GeV. Notice that below the top threshold, the sign of the effect changes. At zero incoming bino momentum, the coupling of the Z to the final state fermions is proportional to T_3^F , as seen in eq. (9). Above the top threshold, zero temperature annihilation is primarily to tops, while below the top threshold it is primarily to b 's and τ 's. Thus $\mathcal{T}_{\text{loop}}(p = 0)$ switches sign, while $\mathcal{T}_{\text{sfex}}(p = 0)$ does not.

Finally in fig. (5), we compare the effect of including the loop diagrams (2) on the zero-temperature cross-section a to the effect of including the higgsino mixing diagram (3). Calling the change in a due to the loop diagrams $\Delta_{\text{loop}}a$ and the change in a due to the higgsino mixture $\Delta_{\text{hm}}a$, we plot $\Delta_{\text{loop}}a/\Delta_{\text{hm}}a$ as a function of ε and $m_{\tilde{B}}$ using $m_{\tilde{F}} = 500$ GeV. As ε becomes large, the effect of the loop correction greatly exceeds the effect of higgsino mixing except very near to the value of $m_{\tilde{B}}$ at which the loop's effect on the cross section vanishes.

To summarize, we have calculated the effect of the loop diagram of fig. (1) on the annihilation cross-section for binos. We find that away from the Z -pole, the effect of the additional diagram is to change the relic density of binos $\Omega_{\tilde{B}}h^2$ by at most a few percent. This is true over the physically allowed range of common sfermion mass $m_{\tilde{F}}$ and bino mass $m_{\tilde{B}}$, though it is larger than contributions from the direct annihilation to Z 's via the small but non-zero admixture of higgsinos in $\tilde{\chi}^0$, typically included in this type of calculation for a wide range in values of the higgsino mixing mass ε . Near the Z -pole, we expect the effect of loop corrections to be considerably larger. The effect of the loop diagram on the zero-temperature cross-section is larger and may be as large as 11%.

Acknowledgements

This work was supported in part by DOE grant DE-FG02-94ER-40823 and NSF grant PHY-91-16964. The work of KAO was in addition supported by a Presidential Young Investigator Award.

References

- [1] A. Dolgov, Phys. Rep. **222** (1992) 309.
- [2] J. Ellis, J. Hagelin, D.V. Nanopoulos, K.A. Olive and M. Srednicki, Nucl. Phys. **B238** (1984) 453.
- [3] K.A. Olive and M. Srednicki, Phys. Lett. **B230** (1989) 78; Nucl. Phys. **B 355** (1991) 208.
- [4] K. Greist, Phys. Rev. **D38** (1988) 2357.
- [5] K. Greist, M. Kamionkowski, and M.S. Turner, Phys. Rev. **D41** (1990) 3565.
- [6] J. McDonald, K.A. Olive, and M. Srednicki, Phys. Lett. **B283** (1992) 80.
- [7] M.M. Nojiri, Phys. Lett. **B261** (1991) 76; J. Ellis and L. Roszkowski, Phys. Lett. **B283** (1992) 252; J. Lopez, D.V. Nanopoulos, and K. Yuan, Nucl. Phys. **B370** (1992) 445; M. Kawasaki and S. Mizuta, Phys. Rev. **D46** (1992) 1634; J. Lopez, D.V. Nanopoulos, and K. Yuan, Phys. Lett. **B267** (1991) 219.
- [8] M. Drees and M.M. Nojiri, Phys. Rev. **D47** (1993) 376.
- [9] T. Falk, R. Madden, K.A. Olive, and M. Srednicki, Phys. Lett. **B318** (1993) 354.
- [10] K. Greist and D. Seckel, Phys. Rev. **D43** (1991) 3191.
- [11] S. Mizuta and M. Yamaguchi, Phys. Lett. **B298** (1993) 120.
- [12] D. Pierce and A. Papadopoulos, hep-ph/9312248; A. B. Lahanas, K. Tamvakis, and N. D. Tracas, hep-ph/9312251.
- [13] M. Srednicki R. Watkins, and K.A. Olive, Nucl. Phys. **B310** (1988) 693.
- [14] M. Srednicki, S. Theissen and J. Silk, Phys. Rev. Lett. **56** (1986) 263; S. Rudaz, Phys. Rev. Lett. **56** (1986) 2188; Phys. Rev. **D39** (1989) 3549; L. Bergstrom and H. Snellman, Phys. Rev. **D37** (1988) 3737; J. Ellis, R. A. Flores, K. Freese, S. Ritz, D. Seckel and J. Silk, Phys. Lett. **B214** (1989) 403; G. F. Giudice and K. Griest, Phys. Rev. **D40** (1989) 2549; A. Bouquet, P. Salati and J. Silk, Phys. Rev. **D40** (1989) 3168; F. Stecker and A. Tylke, Astrophys. J. **343** (1989) 169; S. Rudaz and F. Stecker, Astrophys. J. **368** (1991) 406.

Figure Captions

Fig. 1) Feynman diagrams for loop corrections to $\tilde{B}\tilde{B} \rightarrow Z^*$.

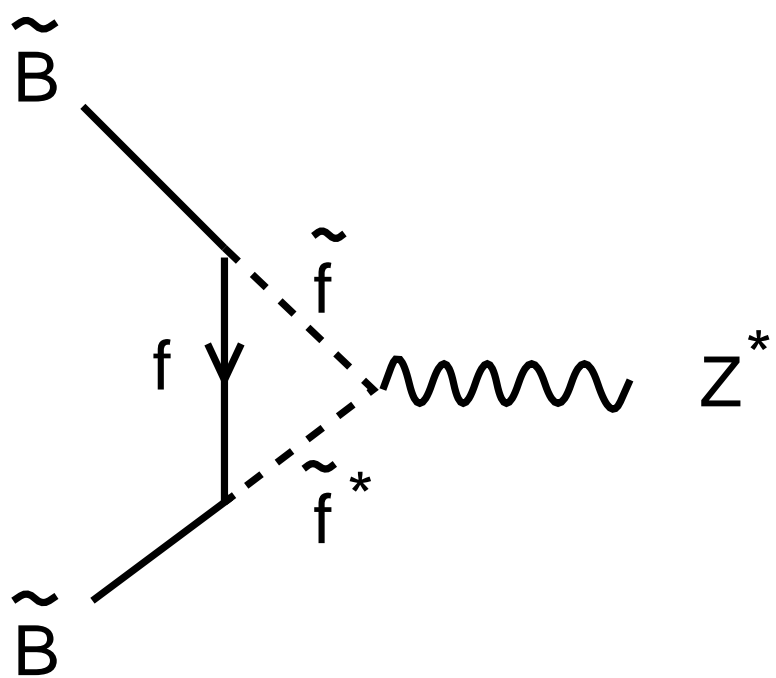
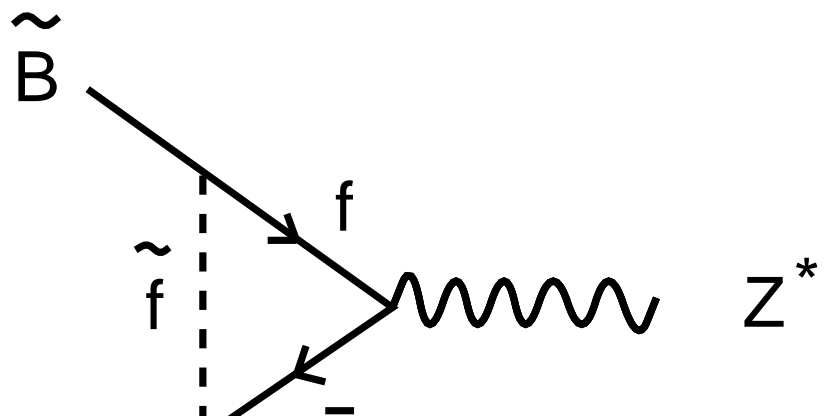
Fig. 2) Relic density $\Omega_{\tilde{B}}h^2$ of binos, assuming bino annihilation only due to sfermion exchange. We take $\tan\beta = 2$, $m_{\text{top}} = 160$ GeV, and a common sfermion mass $m_{\tilde{F}} = m_{\tilde{f}}$.

Fig. 3) A comparison of the effects of the loop diagrams and the higgsino mixing diagram on the relic density of binos $\Omega_{\tilde{B}}h^2$, for several values of ε . In the area to the left of each curve labelled by ε , the loop correction has a greater effect on $\Omega_{\tilde{B}}h^2$ than the higgsino mixing correction.

Fig. 4) The effect of the loop diagrams on the zero-temperature cross-section. Contours label the percentage change in a due to the inclusion of the loop correction.

Fig 5) A comparison of the effects of the loop diagrams and the higgsino mixing diagram on the zero-temperature cross-section.

Fig 1



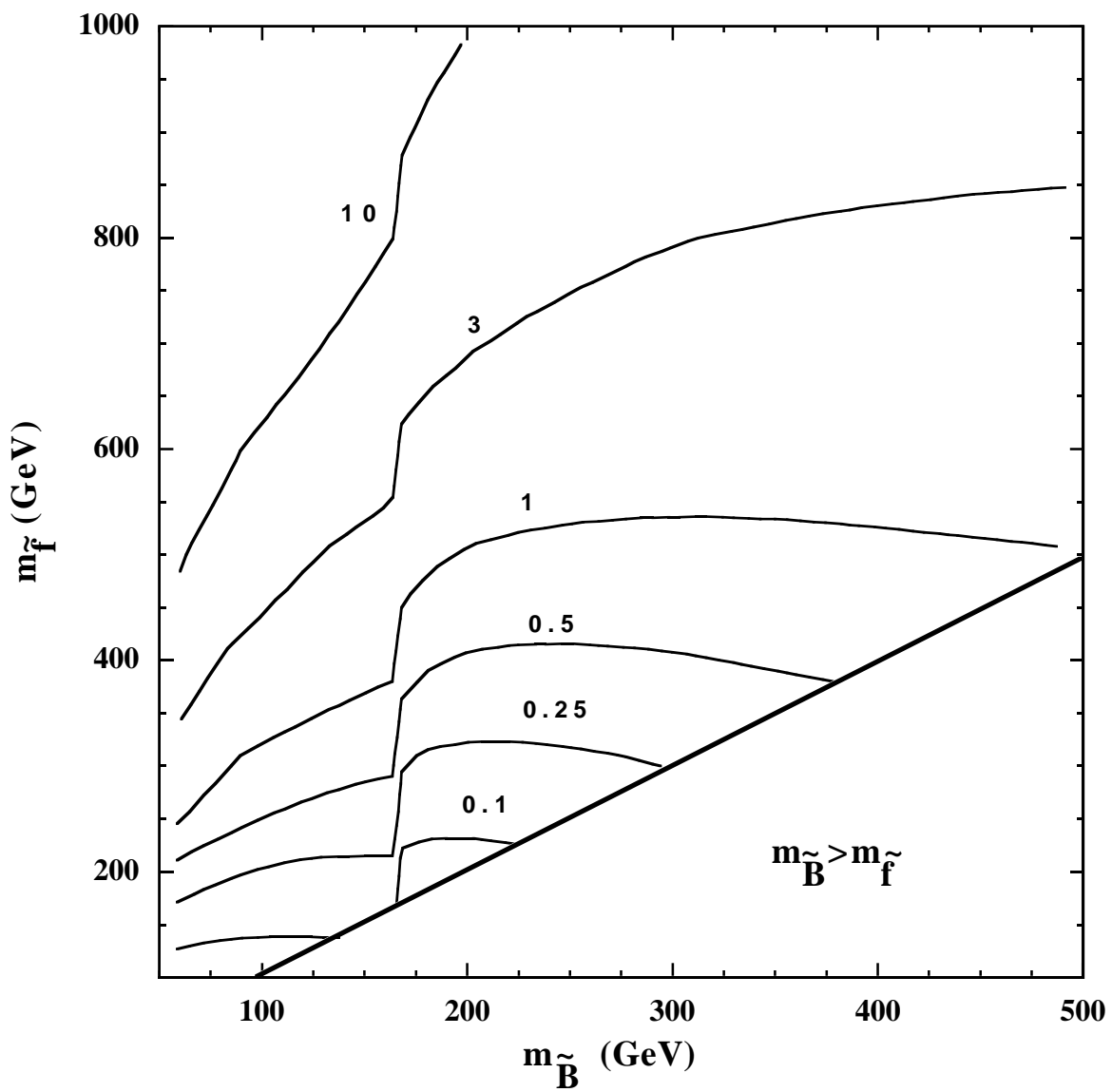
This figure "fig1-1.png" is available in "png" format from:

<http://arxiv.org/ps/hep-ph/9402233v1>

This figure "fig2-1.png" is available in "png" format from:

<http://arxiv.org/ps/hep-ph/9402233v1>

Fig 2



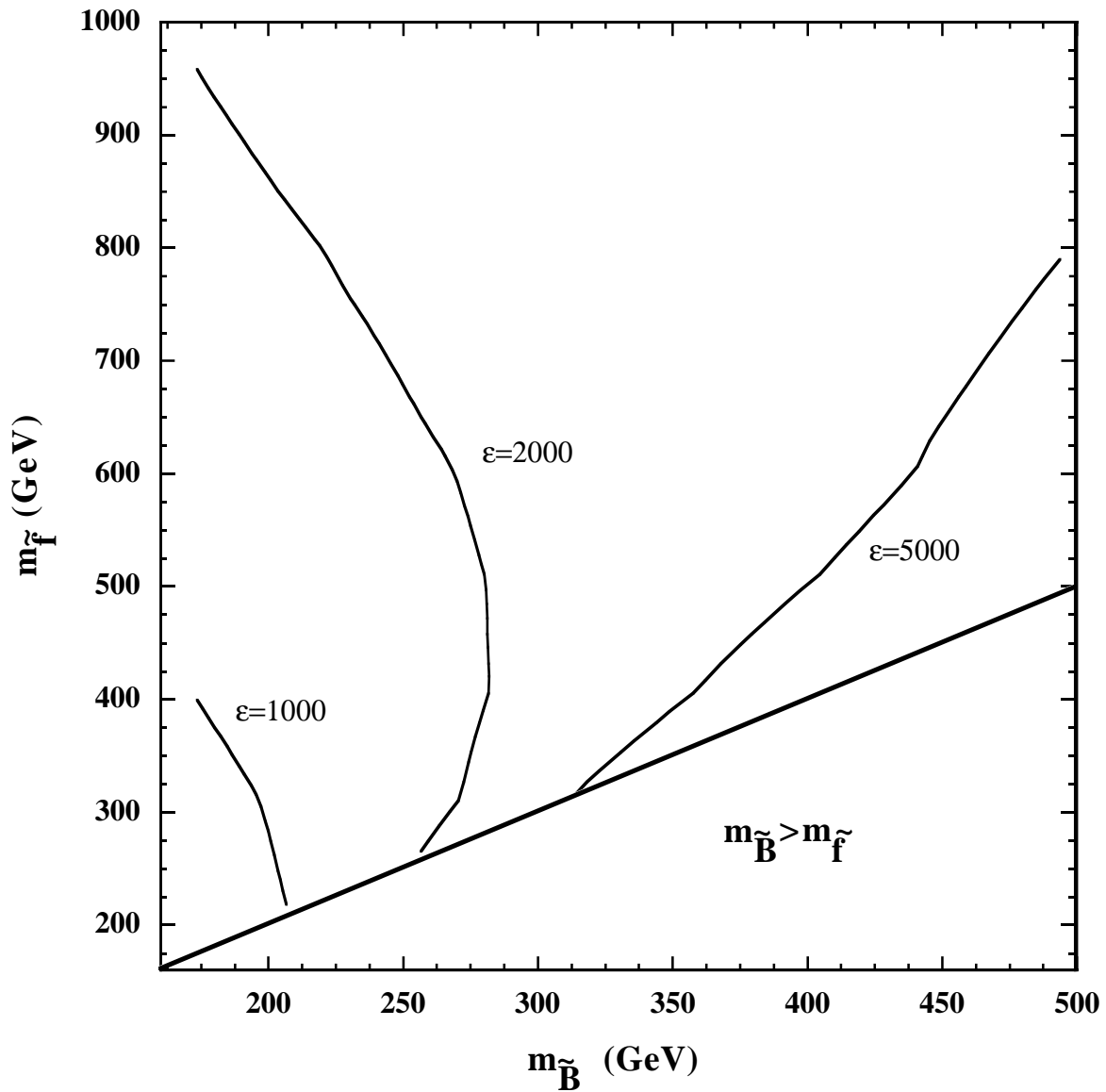
This figure "fig1-2.png" is available in "png" format from:

<http://arxiv.org/ps/hep-ph/9402233v1>

This figure "fig2-2.png" is available in "png" format from:

<http://arxiv.org/ps/hep-ph/9402233v1>

Fig 3



This figure "fig1-3.png" is available in "png" format from:

<http://arxiv.org/ps/hep-ph/9402233v1>

Fig 4

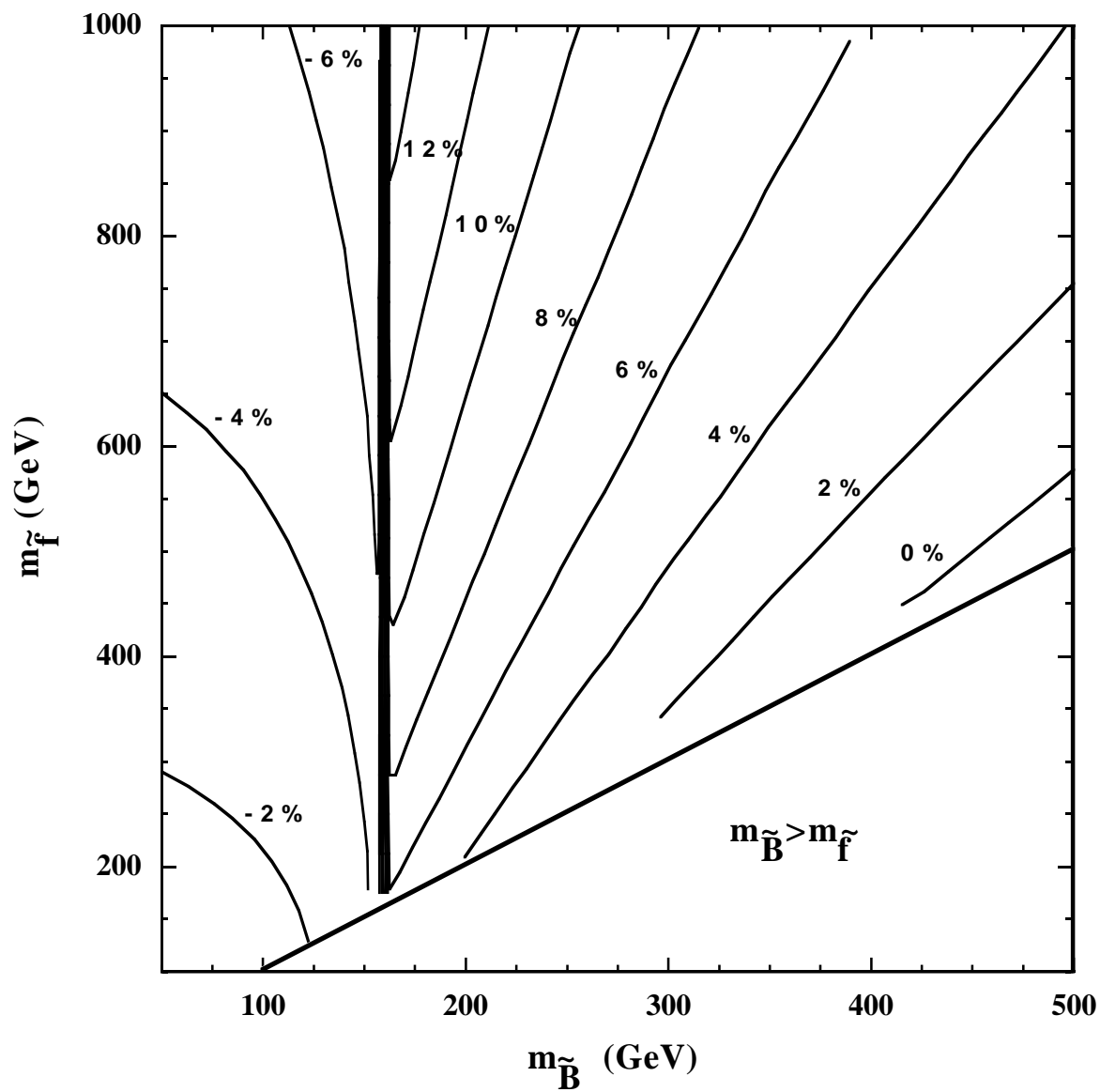


Fig 5

